International Journal of Thermal Sciences 134 (2018) 380–391

Contents lists available at ScienceDirect

International Journal of Thermal Sciences

journal homepage: www.elsevier.com/locate/ijts

Thermal behavior and fluid flow during humping formation in high-speed full penetration gas tungsten arc welding

Xiangmeng Meng, Guoliang Qin*, Ran Zong

Key Laboratory for Liquid-Solid Structural Evolution and Processing of Materials, Ministry of Education, Shandong University, Jinan 250061, PR China

ARTICLE INFO

Keywords:
Humping defect
Thermal behavior
Fluid flow
Gas tungsten arc welding
Full penetration
Modelling

ABSTRACT

An unusual type of humping defect with periodic humped region and perforated region may occur in high-speed full penetration GTAW, which deteriorates the homogeneity of weld property seriously. In this paper, the thermal behavior and fluid flow during full penetration humping (FP-humping) formation is revealed by a numerical investigation to explain the defect's physical mechanism. Self-adaptive double-ellipse distributions of arc heat flux, arc pressure, arc shear stress and electromagnetic force varying with transient free surface evolution are proposed. For the first time, the actual morphology of FP-humping in GTAW can be predicted numerically. The numerical results are well verified by experimental weld geometry and high-speed melt pool images captured by a color camera. The workpiece is melted under arc heat to form the melt pool, and its free surface is gouged significantly under strong arc forces. When the depth of gouging region approaches workpiece thickness, the bottom thin liquid layer in gouging region is easily disrupted to initiate FP-humping formation. The lateral channel becomes the only transfer channel for liquid metal backward flow. The transition region between lateral channel and rear part of melt pool will be necked, and solidified instantly without the arc heat. Both scaling model of thermal conduction and numerical results imply that the premature solidification of necked lateral channel is a predominant factor to influence the FP-humping formation.

1. Introduction

Gas tungsten arc welding (GTAW) is a critical joining technique for metallic material e. g. steel, Al alloy, Mg alloy and nickel alloy in manufacturing industry owing to its high arc stability, reduced spatter, superior weld quality and easy automation. In particular, it is extensively used in thin-walled structure joining, in which single pass full penetration welding is generally required. However, continuous and sound full penetration weld bead may not be obtained in high-current and high-speed category because an unusual type of weld bead defect, namely full penetration humping (FP-humping) or blowhole, easily occurs [1,2]. The FP-humping usually consists of periodically or aperiodically spaced humped region and perforated region. It severely deteriorates the homogeneity and continuity of weld property and may cause stress concentration in the perforated region.

The morphology of FP-humping is distinct from typical humping defect in high-speed welding or burn-through defect in low-speed welding. In comparison to the typical humping defect, the perforated region without any solidified weld metal is through the thickness of workpiece. In comparison of the burn-through defect, the majority of weld metal is accumulated at the front side of weld, rather than the back side. The FP-humping's special morphology implies that it may have the unique formation mechanism which has a close correlation with the heat transfer and fluid flow in melt pool. Quantitative characterization of melt pool behavior can provide a deeper insight for the formation of FP-humping and, correspondingly, offer some helps to eliminate this defect.

The occurrence of FP-humping defect has been reported in GTAW, gas metal arc welding (GMAW), laser beam welding (LBW) and electron beam welding (EBW) [1,2]. Albright and Chiang employed capillary instability theory to explain and predict FP-humping in LBW of stainless steel [3]. When the workpiece was fully penetrated, the melt pool with top and bottom free surfaces was analogous to a cylindrical fluid jet. The melt pool may break into individual droplet under the surface tension force if its length exceeded a critical value. Deutsch et al. suggested that the FP-humping was an indication of excessive heat input in LBW of Al alloy, and formed due to keyhole instability [4]. Kwon and Weckman considered that the FP-humping occurred when surface tension was insufficient to balance with arc force and gravity in the double sided arc welding of plasma arc welding + GTAW [5,6]. Based on the high-speed images of melt pool, the study of Meng et al. indicated that a severely gouged region was formed in melt pool under strong arc force from high

* Corresponding author.
E-mail address: glqin@sdu.edu.cn (G. Qin).

https://doi.org/10.1016/j.ijthermalsci.2018.08.028
Received 28 February 2018; Received in revised form 16 August 2018; Accepted 16 August 2018

welding current, and the liquid metal mainly flowed to the rear region of melt pool through lateral channel in high-speed GTAW. Only an extremely thin liquid layer (less than 200 μm) existed in the gouging region. If the workpiece was fully penetrated, the thin liquid layer was hardly maintained steadily, initiating the FP-humping formation. The scaling analysis suggested that the rapid solidification of lateral channel promoted the subsequent defect formation [7].

Although various theories have been proposed to explain FP-humping formation in different welding processes, the difficulty in experimental measurement of melt pool is still a challenging impediment for rigorous understanding of FP-humping formation. The numerical simulation provides a potential way to acquire accurate data of melt pool behaviors e. g. temperature distribution, fluid flow, free surface evolution etc. Preliminary attempts have been made to investigate the formation mechanism of high-speed weld bead defects such as undercut and typical humping.

The undercut defects in GTAW and GMAW were studied numerically using a heat transfer model with free surface deformation [8,9]. A fuller three-dimensional transient heat transfer and fluid flow model coupled with volume-of-fluid (VOF) method was developed recently to simulate the formation procedure of GTAW undercut [10]. The rapid solidification of periphery part of melt pool and the inward velocity of liquid metal promoted undercut formation. Numerical analyses were also performed for humping phenomena in high-speed direct current or pulsed GMAW process [11–13], and for suppression measures by Laser + GMAW or twin wire GMAW [14,15]. The capillary instability and rapid solidification of necked channel were revealed to be responsible for humping occurrence. In addition, Meng et al. and Otto et al. established numerical models of high-speed GTAW and LBW, respectively, to calculate the heat transfer and fluid flow of melt pool during humping formation [16,17]. It can be concluded from the numerical studies that both the thermal and flowing factors are involved in the occurrence of high-speed weld bead defects. However, a critical review of literature shows that the existing numerical studies about humping defect mainly focus on partial penetration condition. The simulation work about FP-humping has not been reported.

What is necessary but not available now is a comprehensive and quantitative understanding of physical mechanism of FP-humping defect. The objective of this study is to rationalize the formation of FP-humping in high-speed GTAW through numerical modelling. A three-dimensional transient computational fluid dynamics (CFD) model coupled with VOF algorithm is developed to calculate temperature and velocity fields in melt pool, free surface deformation and solidified weld geometry. The numerical model is well validated by comparison with experimental weld geometry and high-speed images of melt pool. The formation process of FP-humping is analyzed using the numerical data assisted by parametric experiment and high-speed camera imaging. The initial factor and dominant factor for FP-humping are discussed and identified.

2. Experimental procedure

The ASTM 409L stainless steel plate was used as base metal, and the dimension was 300 × 60 × 1.5 mm. Table 1 gives the nominal chemical compositions of 409L steel. A DC inverter power sources with 500 A capacity was used as welding power supply. Bead-on-plate configuration were implemented and the direct current electrode negative (DCEN) mode was chosen. The detailed welding parameters are shown in Table 2, which was determined according to the authors' preliminary work [7].

Table 1
Nominal chemical compositions of 409L ferritic stainless steel (wt %).

C	Mn	Cr	Ni	S	Si	P	N	Ti	Cu	Fe
0.013	0.34	11.32	0.08	0.005	0.45	0.016	0.014	0.201	0.02	Bal

Table 2
Welding parameters used in experiment and simulation.

Welding parameters	Values
Welding current (A)	350
Welding speed (m/min)	1.6–2.0
Arc voltage (V)	17.2
Electrode material	Thoriated tungsten electrode (2% thorium)
Electrode diameter (mm)	3.2
Electrode angle	Vertical to base metal
Electrode tip angle (deg)	30
Electrode height (mm)	2
Shielding gas	Pure argon, 15L/min

An image acquisition system consisting of a high-speed color camera with 100 fps framing rate (DS-UN1401) and a PC with data acquisition card was established to capture the real time melt pool shape. In order to suppress the intensive arc interference on imaging signal and to obtain clear images of rear melt pool, a neutral filter was used to cover part of the lens [18]. The principal optic axis of the camera was perpendicular to the welding direction and 40 deg to the welding plane. A schematic of the experimental system is shown in Fig. 1.

The macro- and micro-structure observations of weld were performed using optical microscope (Zeiss Stemi DV4). The specimens were prepared following the standard of ASTM E3-11 and etched with a solution of nitric acid, hydrochloric acid and distilled water in 1:1:1 ration for10 s.

3. Mathematical modelling

The nomenclatures used are listed in Table 3. The transport phenomena of melt pool in the high-speed GTAW are extremely complicated and with multiple couplings. To make the problem tractable and reduce the computational intensity, some simplifications are made in this paper [19]:

(1) The molten metal is laminar, Newtonian and incompressible fluid. Boussinesq approximation is employed to treat the buoyancy term.
(2) The thermal conductivity, specific heat, viscosity and surface tension coefficient of 409L steel are temperature dependent, and other physical properties are constant.
(3) Only half of workpiece is taken as computational domain considering the symmetry with respect to the welding line.

3.1. Governing equations

With the above assumptions, the governing equations in fixed Cartesian coordinate can be expressed as follows.

Continuity equation

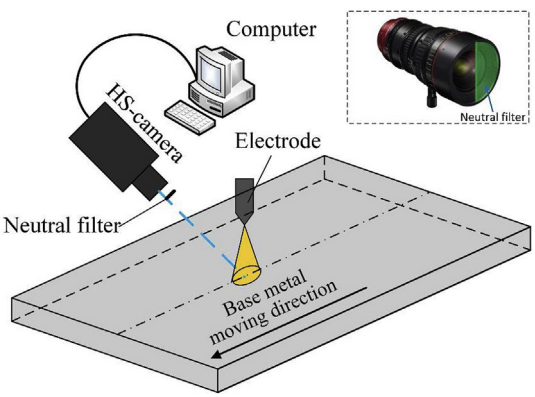

Fig. 1. Schematic of GTAW and high-speed image acquisition system.